

Tight cosmological constraints from the angular-size/redshift relation for ultra-compact radio sources

J C Jackson^{yz}

^y Division of Mathematics and Statistics, School of Informatics, Northumbria University, Ellison Place, Newcastle NE1 8ST, UK

Abstract.

Some years ago (Jackson and Dodgson 1997) analysis of the angular-size/redshift relationship for ultra-compact radio sources indicated that for spatially flat universes the best choice of cosmological parameters was $\Omega_m = 0.2$ and $\Omega_\Lambda = 0.8$. Here I present an astrophysical model of these sources, based upon the idea that for those with redshift $z > 0.5$ each measured angular size corresponds to a single compact component which is moving relativistically towards the observer; this model gives a reasonable account of their behaviour as standard measuring rods. A new analysis of the original data set (Gurvits 1994), taking into account possible selection effects which bias against large objects, gives $\Omega_m = 0.24 \pm 0.09 = 0.07$ for flat universes. The data points match the corresponding theoretical curve very accurately out to $z \approx 3$, and there is clear and sustained indication of the switch from acceleration to deceleration, which occurs at $z = 0.85$.

1. Introduction

The default cosmological paradigm now is that we are living in a spatially flat accelerating Universe with matter (baryons plus Cold Dark Matter) and vacuum density-parameters $\Omega_m = 0.27$ and $\Omega_\Lambda = 0.73$ respectively, known as the concordance model. Definitive confirmation of a consensus which has been growing over the last two decades came with the recent Wilkinson Microwave Anisotropy Probe (WMAP) results (Spergel et al 2003). The original evidence for such models was circumstantial, in that they reconcile the inflationary prediction of flatness with the observed low density of matter (Peebles 1984; Turner et al 1984). The first real evidence came from observations of very large-scale cosmological structures (Efsthathiou et al 1990), which paper clearly advocated everything that has come to be accepted in recent times: "...very large scale cosmological structures can be accommodated in a spatially flat cosmology in which as much as 80 percent of the critical density is provided by a positive cosmological constant. In such a universe expansion was dominated by CDM until a recent epoch, but is now governed by the cosmological constant." A similar case for this model was made by

^z To whom correspondence should be addressed (jhn.jackson@unn.ac.uk)

Ostriker and Steinhardt (1995), who also noted that the location and magnitude of the first Doppler peak in the cosmic microwave background (CMB) angular spectrum was marginally supportive of flatness. However, the paradigm did not really begin to shift until the Hubble diagram for Type Ia supernovae (SNe Ia) (Schmidt et al 1998; Riess et al 1998; Perlmutter et al 1999) provided reasonably convincing evidence that $\Omega_m > 0$; the corresponding confidence region in the Ω_m - Ω_Λ plane was large and elongated, but almost entirely confined to the positive quadrant. The dramatic impact of these results was probably occasioned by the simple nature of this classical cosmological test; coupled with accurate measures of the first Doppler peak in the CMB angular spectrum (Balbi et al 2000; de Bernardis et al 2000; Hanany et al 2000), which established flatness to a high degree of accuracy, the SNe Ia results made anything but the concordance model virtually untenable. This paper is in part retrospective, and is about another simple classical cosmological test. Some years ago we published an analysis of the angular-size/redshift diagram for millisecond radio-sources (Jackson and Dodson 1997; see also Jackson and Dodson 1996), with a clear statement to the effect that "if the Universe is spatially flat, then models with low density are favoured; the best such model is $\Omega_m = 0.2$ and $\Omega_\Lambda = 0.8$ ". This result pre-dates the SNe Ia ones.

Ultra-compact radio sources were first used in this context by Kellermann (1993), who presented angular sizes for 79 objects, obtained using very-long-baseline interferometry (VLBI). These were divided into 7 bins according to redshift z , and the mean angular size plotted against the mean redshift for each bin. The main effect of Kellermann's work was to establish that the resulting θ - z relationship was compatible with standard Friedmann-Lemaître-Robertson-Walker (FLRW) cosmological models, in sharp contrast to the case for the extended radio structures associated with radio-galaxies and quasars. In the latter case typical component separations are 30 arcseconds, and the observed relationship is the so-called Euclidean curve $\theta \propto 1+z$ (Legg 1970; Miley 1971; Kellermann 1972; Wardle and Miley 1974); this deficit of large objects at high redshifts is believed to be an evolutionary effect, brought about by interaction with an evolving extra-galactic medium (Miley 1971; Barthel and Miley 1988; Singal 1988), or a selection effect, due to an inverse correlation between linear size and radio power (Jackson 1973; Richter 1973; Masson 1980; Nilsson et al 1993). However, see Buchalter et al (1998) for a significant attempt to disentangle these effects. Ultra-compact objects have short lifetimes and are much smaller than their parent active galactic nuclei (AGNs), so that their local environment should be free of cosmological evolutionary effects, at least over an appropriate redshift range. However, it is not clear that observations of these objects are completely free from selection effects.

Kellermann's work was extended by Gurvits (1994), who presented a large VLBI compilation, based upon a 2.3 GHz survey undertaken by Preston et al (1985), comprising 917 sources with a correlated flux limit of approximately 0.1 Jy; the subsample selected by Gurvits comprises 337 sources with known redshifts, and objective measures of angular size based upon fringe visibility (Thompson, Moran and Swenson 1986). Gurvits gave good reasons for ignoring sources with $z < 0.5$, and using just

the high-redshift data found marginal support for a low-density FLRW model, but considered only models with $\Omega_m = 0$. Jackson and Dodgson (1997) was based upon Gurvits' sample, and considered 256 sources in the redshift range 0.511 to 3.787, divided into 16 bins of 16 objects. More recently Gurvits et al (1999) have presented a new compilation of 330 compact radio sources, observed at a somewhat higher frequency ($\nu = 5$ GHz), which has stimulated a number of analyses (Vishwakarma 2001; Cunha et al 2002; Lima and Alcaniz 2002; Zhu and Fujimoto 2002; Chen and Ratra 2003; Jain et al 2003), which consider the full Ω_m plane and/or alternative models of the vacuum. However, the constraints placed upon cosmological parameters by this later work are significantly weaker than for example the SNe Ia constraints alone, and very much weaker than those obtained when the latter are coupled with CMB and Large Scale Structure observations (Efstathiou et al 1999; Bridle et al 1999; Lasenby, Bridle and Hobson 2000; Efstathiou et al 2002).

The main purpose of this work is to show that angular-size/redshift data relating to these sources place significant constraints upon cosmological parameters, comparable with those due to any of the currently fashionable tests taken in isolation, and also to establish a plausible astrophysical model which gives them credibility as putative standard measuring rods. I find that the original Gurvits (1994) compilation better in this respect than the later one due to Gurvits et al (1999), and I shall eventually discuss why this might be so. The astrophysical model and associated selection effects are discussed in Section 2, where evidence of such an effect is found. Appropriate countermeasures are discussed in Section 3; these have some similarities to the scheme adopted by Buchalter et al (1998) with regard to the extended radio sources, and the parallels will be discussed. The corresponding cosmological results are presented as marginalized confidence regions in the Ω_m plane, with some consideration of the quintessence parameter w . It is in these considerations that this work is new, and differs significantly from the analysis of essentially the same data in Jackson and Dodgson (1997). At this stage I make no attempt to combine these data with other observations, being content to show that the former deserve to be part of the cosmological canon. Quoted figures which depend upon Hubble's constant correspond to $H_0 = 100 \text{ km sec}^{-1} \text{ Mpc}^{-1}$.

2. Selection effects and a source model

In a flux-limited sample sources observed at large redshifts are intrinsically the most powerful, so that an inverse correlation between linear size and radio luminosity will introduce a bias towards smaller objects. There are several reasons for expecting such a correlation. On quite general grounds we would expect sources to be expanding, and their luminosities to decrease with time after an initial rapid increase (Jackson 1973; Baldwin 1982; Blundell and Rawlings 1999). Additionally, Doppler beaming from synchrotron components undergoing bulk relativistic motion towards the observer is known to be important in compact sources, and Dabrowski et al (1995) have argued

that this will introduce a similar correlation. Doppler boosting was first discussed by Shklovsky (1964a,b), to explain the apparently one-sided jet in M 87. Subsequently Rees (1966) devised a relativistically expanding model with spherical symmetry, to account for the rapid variability observed in powerful radio sources, and noted that apparently superluminal motion should be seen in such models, some ten years before this phenomenon was observed (Cohen 1975; Cohen et al 1976, 1977). Shklovsky's basic twin-jet model has been the subject of many elaborations over the past three decades, and Doppler boosting is now the basis of the so called unified model of compact radio sources, in which orientation effects in an essentially homogeneous population generate the full range of observed properties. The notion that quasi-stellar radio sources are just a small subset of apparently radio-quiet quasi-stellar objects, that is those which are viewed in the appropriate orientation, was first discussed by Scheuer and Readhead (1979), and subsequently by Orr and Browne (1982), who considered the relative frequencies of the two classes. Particularly germane to the discussion below are Blandford and Königl (1979a), Blandford and Königl (1979b) and Lind and Blandford (1985). This is not intended to be a comprehensive historical review, examples of which can be found in Blandford et al (1977) and Kellermann (1994).

The underlying source population probably consists of compact symmetric objects (CSOs), of the sort observed by Wilkinson et al (1994) at moderate redshifts ($0.2 < z < 0.5$), with radio luminosity densities of several times $10^{26} \text{ W Hz}^{-1}$ at 5 GHz; these comprise central low-luminosity cores straddled by two mini-lobes, the former contributing no more than a few percent of the total luminosity (Readhead et al 1996a); without Doppler boosting these objects would be too faint to be observed at higher redshifts. It is thus reasonable to suppose that in the most distantly observed cases the lobes are moving relativistically and are close to the line of sight. For this reason the use of ultra-compact sources as standard measuring rods has been questioned by Dabrowski et al (1995), who consider a simple model, comprising two identical but oppositely directed jets (treated as point or line sources), and assume that the measured angular size corresponds to their separation projected onto the plane of the sky; thus apparent radio power increases and angular size decreases as the beams get closer to the line of sight. However, this model is not realistic, as the counter-jet would be very much fainter than the forward one, for example by a factor of up to 10^6 for a jet Lorentz factor

of 5. It is more reasonable to suppose that we observe just that component which is moving relativistically towards the observer, and in particular that the interferometric angular sizes upon which this work is based correspond to the said components.

It is reasonable to ask if the above supposition is compatible with VLBI images of distant AGNs and quasars. At first sight this is not the case; it is well-known that these images typically show a core/one-sided jet structure (see for example Taylor et al 1996), rather than a single component. However, it is well-known that there is an inconsistency here, if the cores are to be identified with those of the underlying CSO population and the latter are unbeamed. The problem then is that as mentioned above members of the CSO population are typically jet dominated, and would become

distinctly more so when viewed close to the jet axis, by several orders of magnitude, which is not what is observed; in VLBI images of distant sources the core is usually dominant, and the jet is often absent. This dilemma has been resolved by Blandford and Königl (1979a,b), who describe a model in which the 'core' is really part of the jet, and is thus also Doppler boosted (see also Kellermann 1994). In their model the core emission originates in the stationary compact end of a quasi-steady supersonic jet, where the latter becomes optically thick; the so called jet emission comes from up-stream shock waves associated with dense condensations within the bulk flow which are being accelerated by the latter. A stationary core which is nevertheless relativistic is necessary, to reconcile superluminal expansion with the observed relative fluxes from the two components. In the latter respect it is essential that $\beta_j < \beta_c$ (where subscripts c and j denote core and jet respectively), but this is part of the Blandford and Königl (1979a,b) model; jet domination then changes into core domination as θ changes from $\theta = 2$ to zero, where θ be the angle between the jet axis and the line-of-sight; the transverse Doppler effect diminishes the core relative to the jet when $\theta = 2$, but the roles are reversed when $\theta = 0$. In other words the core emission is more beamed than that of the jet.

If the two components have flat spectra and the same rest-frame luminosities, and $R(\theta)$ is the core/jet luminosity ratio, then

$$R(0) = \frac{L_c}{L_j} \quad \text{and} \quad R(\theta = 2) = \frac{L_j}{L_c} \quad (1)$$

and the crossover angle at which $R = 1$ is $(\beta_j \beta_c)^{1/2}$ (see below for the definition of n). A ratio $\beta_c = \beta_j^2$ to 3 would effect a transition of the correct magnitude; for typical values of β the crossover angle is 15 to 20°.

If the basic model outlined above is correct, one consequence is that statistically cores are observed at something like a fixed rest-frame frequency; suppose that a core has rest-frame luminosity density L , with flat spectral index $\alpha = 0$ characteristic of ultra-compact sources. The Doppler boosting factor D is

$$D = \gamma^{-1} (1 - \beta \cos \theta)^{-1} \quad (2)$$

where β is the object velocity in units of c , and as above θ is the angle between this velocity and the line of sight. For a source at redshift z and angular-diameter distance $D_A(z)$, the observed flux density S is thus

$$S = \frac{L D^n}{4 (1+z)^n D_A^2} \quad \text{and} \quad \frac{D}{1+z} = \frac{4 D_A^2 S^{1/n}}{L} (1+z)^{(3-n)/n} \quad (3)$$

where $n = 3$ for discrete ejecta and $n = 2$ for a continuous jet (Lind and Blandford 1985). As we have seen, in reality the situation lies between these two extremes, and a value $n = 5/2$ will be used for purposes of illustration. In the redshift range of interest $D_A(z)$ is close to its minimum, and is thus a slowly varying function of z , so that for an object observed close to the flux-limit the ratio $D/(1+z)$ is proportional to $(1+z)^{1/5}$ and is roughly fixed: the survey frequency of 2.3 GHz corresponds to a rest-frame frequency

of 2.3 GHz divided by this ratio, which would for example greatly reduce the effect, deleterious in this context, of any dependence of linear size on rest-frame frequency. Similar considerations apply to jets if $\beta = c$ is fixed.

It has been noted by Frey and Gurvits (1997) that jets become noticeably less prominent, in terms of both morphology and luminosity, as redshift increases. At $z > 3$ jets appear to be absent or vestigial (see for example the VLBI images presented by Gurvits et al 1994, Frey et al 1997 and Paragi et al 1999). Frey and Gurvits (1997) reasonably attribute this phenomenon to differential spectral properties, cores being brighter than the jets in this respect. However, if statistically the cosmological redshift is roughly cancelled out by the Doppler boost, as suggested in the last paragraph, then spectral differences should not be as important as Frey and Gurvits (1997) suppose. In part the phenomenon is probably the Dabrowski et al (1995) selection effect in operation: the viewing angle gets smaller as z increases, and projection effects mean that the two components first overlap and then become superimposed, when we see a single composite source. Such selection is thus not as significant as Dabrowski et al (1995) suggest, particularly at high redshifts, because the components are not point sources, and angular sizes do not vanish as the beams get closer to the line of sight. At lower redshifts we see more structure; cursory inspection of 113 VLBI images (not redshift selected) presented by Taylor et al (1996) suggests that about one third of these are superimposed composites, one third are core/jet overlaps, and one third show two separate components forming more complex structures. However, Dabrowski et al (1995) show that their effect is not significant at low redshifts, typically $z < 1.5$ for the flux limit of 0.1 Jy which characterises this sample. Thus over the full redshift range it is reasonable to suppose that this particular selection is of marginal importance. The matter will be discussed further, when suitable countermeasures are considered. Although these considerations are interesting from an astrophysical point of view, their significance here is to identify these superimposed core/jet composites as the components which in effect determine the measured angular sizes upon which this work is based.

Finally, with regard to establishing ultra-compact sources as standard linear measures, I note that the parent galaxies in which they are embedded are giant ellipticals, with masses close $10^{13} M_{\odot}$; it is known that their central black holes have masses which are tightly correlated with this mass (Kormendy 2001a,b), being 0.15% of same, close to $1.5 \times 10^{10} M_{\odot}$. The central engines which power these sources are thus reasonably standard objects.

The question of whether there is a linear-size/luminosity correlation of the sort discussed at the beginning of this section is easily settled; Figure 1 is a plot of linear extent d (as indicated by the measured angular size) against correlated rest-frame luminosity L (attributable to the compact component, and calculated assuming isotropic emission and a spectral index $\alpha = 0.1$, where $L \propto \nu^{-\alpha}$), for a selection of redshift bins, each containing 16 sources from the Gurvits (1994) sample. A cosmology is needed for this plot, and I have pre-empted the results to be presented here by using $\Omega_m = 0.24$ and $\Omega_{\Lambda} = 0.76$; however, the significant qualitative aspects of the arguments I shall

present are not sensitive to this choice. There is clear evidence that at any particular epoch individual luminosities are a function of size, and that for sources with $z > 0.2$ this relationship is an inverse correlation. For $z > 0.5$ the relationship is well-represented by

$$L / d^a \quad (4)$$

where in round figures $a = 3$. In the above model, this behaviour would be attributed to expansion of each relativistic component as it moves away from the central engine and grows weaker. However, as noted by Gurvits (1994), the remarkable feature of this diagram is that for $z > 0.5$ there is no marked change in mean size at a given luminosity, over a range of the latter variable which covers three orders of magnitude, which suggests that these two parameters are decoupled. This behaviour is quite compatible with the model outlined above; a tentative subdivision is that for $z < 0.2$ these sources are intrinsically small and weak and not relativistic; between $z = 0.2$ and $z = 0.5$ there is a transitional regime, during which the intrinsic luminosity rises to several times $10^{26} \text{ W Hz}^{-1}$; thereafter the latter is approximately fixed, the sources are ultra-relativistic, and the luminosity range is accounted for largely by changes in Doppler boost. For example with fixed $\delta = 5$, a luminosity boost factor $D^{2.5}$ varies by a factor of 316 as δ changes from 0 to 35. A similar phenomenon has been noted in X-ray astronomy (Fabian et al 1997).

The sub-division outlined above is analogous to the division of extended double radio sources into Fanaro-Riley types I and II (FR-I and FR-II) (Fanaro and Riley 1974; Kembhavi and Narlikar 1999). The radio morphologies of FR-I sources typically show a relatively bright central core from which bright opposed jets emanate in symmetric fashion, which jets terminate in faint diffuse lobes as they run into the intergalactic medium. FR-II sources typically comprise a relatively faint core with a one-sided jet which terminates in a bright compact lobe, with a comparable lobe on the opposite side of the core, but no sign of a corresponding counter-jet; presumably the latter is invisible due to beaming. FR-I sources are relatively weak, having radio luminosities $L(2.3 \text{ GHz}) < 2 \times 10^{24} \text{ W Hz}^{-1}$, whereas FR-II sources are intrinsically strong, having luminosities greater than this figure. Although this threshold luminosity is two orders of magnitude lower than the luminosities associated with the CSOs observed by Wilkinson et al (1994), it may be that the analogy is exact, in that latter are the precursors of FR-I objects, if luminosity evolution is invoked (Readhead et al 1996b). Similarly, the more distant compact objects discussed here may be the precursors of FR-II sources.

Buchalter et al (1998) select FR-II sources as the basis of their work on the angular-size/redshift relation, in part because their morphology allows an objective definition angular size. This selection was effected by choosing sufficiently powerful sources having $z > 0.3$ and the correct radio morphology. Buchalter et al (1998) must then first allow for a lower size cut-off, below which the FR-I/FR-II classification is beyond the resolving power of the instruments in question. Finally Buchalter et al (1998) allow for a linear-size/redshift correlation of the sort discussed above, by assuming $d / (1+z)^c$ and allowing the data to fix the constant c , which represents a combination of several

effects. Such measures appear to be necessary, if the angular-size/redshift diagram for extended sources is to be in concordance with acceptable FLRW cosmological models, but the situation is then too degenerate to make definitive statements about cosmological parameters. As we shall see in the next section, milliarseconds sources are more robust in this respect, and although similar measures will be introduced, they are a refinement rather than a necessity.

Because we cannot measure absolute visual magnitudes or linear sizes directly, it is essential to have a model which supports the choice of the objects in question as standard candles or standard measuring rods. In the case of Type Ia supernovae such support is provided by a reasonably well-established model, based upon accreting Chandrasekhar-mass white dwarfs in binary systems (Branch et al 1995; Livio 2001). I believe that the above model provides similar support for powerful ultra-compact radio sources and the angular-size/redshift diagram.

3. Cosmological parameters

As in Gurvits (1994) and Jackson and Dogson (1997), I shall consider only those sources with $z > 0.5$, amply justified by the discussion above. It is clear that as individual objects these do not have fixed linear dimensions, and we must consider the population mean. Accordingly, the sources are placed in redshift bins, and earlier practice would be to plot simple means for each bin in a $\{z$ diagram. However, due to the selection biases discussed in Section 2, a growing proportion of the larger members of this population will be lost as redshift increases, and simple means introduce a systematic error. According to the adopted model, the effect can be quantified. The flux limit S_c sets a cut-off size d_c at each redshift, such that sources larger than d_c are too faint to be observed. Again taking a flat spectrum, equations (3) and (4) with $a = 3$ give

$$d_c \propto \frac{D^{n=3}}{(4 D_A^2 S_c)^{1/3} (1+z)} : \quad (5)$$

Thus assuming that there is a largest boost factor D which does not change with redshift, and noting that in the redshift range of interest $D_A(z)$ is close to its minimum, we find

$$d_c \propto (1+z)^{-1} : \quad (6)$$

Figure 2 is a plot of linear extent against z for all 337 sources in the Gurvits (1994) sample. The dashed line shows $d_c(z)$ according to equation (6), normalized to give $d_c = 20$ pc at $z = 1$. Figure 2 appears to show that the larger objects are being lost when z exceeds 1.5, in a manner which is in reasonable accord with equation (6). I have adopted the following pragmatic procedure to reduce the concomitant systematic error; instead of simple means I have defined a lower envelope for the data. An obvious choice would be the lowest point within each bin, but this is too noisy. I have defined the lower envelope as the boundary between the bottom third and the top two thirds of the points within each bin, in other words a median which gives more weight to the smaller

objects. Note however that this prescription is not tied to the particular model of bias discussed in Section 2; it is an empirical measure based upon the observation that larger sources appear to be weaker, and its effect would be neutral otherwise. (Gurvitis et al (1999) use ordinary median angular sizes rather than means, to reduce the influence of outliers, which is an added benefit here.) Figure 3 shows 6 weighted median points; each of these derives from a bin containing 42 objects, being the mean of points 11 to 17 within each bin, counting from the smallest object; the sample thus comprises 252 objects in the range $0.541 < z < 3.787$. Error bars are one standard deviation as determined by the said points; they are shown as an indication of the efficacy of this definition of lower boundary, and are not used in the statistical analysis which follows. I have experimented with various bin sizes; the reasons for this particular choice will be discussed later. In all cases means are means of the logarithms.

A simple three-parameter least-squares fit to the points in Figure 3 gives optimum values $m = 0.29$, $\alpha = 0.37$ and mean size $d = 5.7$ parsecs. If the model is constrained to be flat, then a two-parameter least-squares fit gives optimum values $m = 0.24$, $\alpha = 1$, $m = 0.76$ and $d = 6.2$ parsecs, which model is shown as the continuous curve in Figure 3; the latter also shows the zero-acceleration model $m = 0$, $\alpha = 0$, $d = 6.2$ pc as the dashed curve. The difference $\log(\chi^2)$ between the two curves is presented in Figure 4, which shows clearly the shift from acceleration to deceleration. Note however that the actual switch occurs before the crossing point, at $z = (2 - m)^{1/3} - 1 = 0.85$ in this case, roughly where the continuous curve begins to swing back towards the dashed one. Figure 4 establishes definitively and accurately that there is no need to invoke anything other than a simple m model to account for the data, out to a redshift $z = 2.69$. The current record for SNe Ia is SN 1997 at $z = 1.7$ (Gilliland and Phillips 1998; Riess et al 2001), with a somewhat uncertain apparent magnitude.

In order to derive confidence regions, I have defined a fixed standard deviation to be attached to each point in Figure 3: $\sigma^2 = \text{residual sum-of-squares}/(n - p)$, where $n = 6$ is the number of points and $p = 3$ is the number of fitted parameters, giving $\sigma = 0.0099$ in \log in this case. This value of σ is used to calculate χ^2 values at points in a suitable region of parameter space. Figure 5 shows confidence regions in the m plane derived in this manner, marginalized over d according to the scheme outlined in Press et al (1986). Without the extra constraint of flatness little can be said about α , which degeneracy is due to the lack of data points with $z < 0.5$ (Jackson and Dodgson 1996). Nevertheless Figure 5 clearly constrains m to be significantly less than unity. Figure 5 is essentially a refined and tighter version of the diagram presented in Jackson and Dodgson (1997); the significant change is that flat models are now well within the 68% confidence region, whereas previously the figure was 95%; this change is entirely due to the measures relating to selection effects. In the case of flat models, two-dimensional confidence regions can be presented without marginalization. Figure 6 shows such regions in the m plane; marginalizing over d gives 95% confidence limits $m = 0.24 + 0.09 = 0.33$.

With respect to choice of redshift binning the balance is between many bins containing few objects and a small number containing many objects; the former gives poor estimates of population parameters within each bin, but a large number of points to work with in Figure 3; the latter gives better estimates of these parameters but fewer points in Figure 3. I have experimented with 15 bin sizes, from 17 bins of 15 objects to 4 bins of 57 objects, in steps of 3 objects; in each case I have used the largest number of bins compatible with having no objects with $z > 0.5$. I find that the central figure is quite robust, but that accuracy increases gradually as the number of bins is reduced, the best compromise being the one used above. As a check I have calculated the best cosmological parameters in each of the 15 cases, and when selection effects are allowed for I find a mean value $\Omega_m = 0.25$ in the flat case, with 95% confidence limits of 0.06 . If selection effects are ignored corresponding figures are virtually the same, $\Omega_m = 0.24 \pm 0.04$, again in the flat case. However, this coincidence understates the value of the measures relating to selection bias; as mentioned above, these bring flat models well within the 68% confidence region in Figure 5, and more importantly they reveal the expected minimum angular size in Figure 3 (Hoyle 1959).

As already noted with respect to Figure 4, simple Ω_m models give an excellent fit to the data. Nevertheless, in conclusion I consider the limits placed upon the quintessence parameter w , defined by postulating an equation of state for the vacuum of the form $p_{vac} = wp_{vac}$ relating the vacuum density ρ_{vac} to the vacuum pressure p_{vac} , with $|w| \leq 1$ and $w = -1$ corresponding to the conventional vacuum defined by a cosmological constant. For flat models we have a three-parameter system comprising Ω_m, w and d , the quintessence parameter q being $1 - \Omega_m$; we proceed by marginalising over d to give the two-parameter confidence regions shown in Figure 7. The system is highly degenerate, and with respect to material content cannot distinguish between for example a two component mix with $\Omega_m = 0.24, q = 0.76, w = -1$ at one extreme, and a single component compromise with $\Omega_m = 0, q = 1, w = -0.37$ at the other. Lacking any compelling evidence to the contrary, the sensible choice is to retain local Lorentz invariance and assume that $w = -1$.

4. Conclusions

The prescription adumbrated here has produced a set of data points which are remarkably consistent with Ω_m FLRW cosmological models, but there is extensive degeneracy due to the restricted redshift range. This degeneracy is resolved by combining angular-size/redshift data with that CMBR information which indicates flatness, and the two data sets together give $\Omega_m = 0.24 \pm 0.09 = 0.07$. This compares well with the figure $\Omega_m = 0.27 \pm 0.04$ arising from WMAP measurements combined with a host of other astronomical data sets (Spergel et al 2003); the points generated in this work might be added as an extra data set; for future reference these are given in Table 1.

This work builds upon the earlier work of Jackson and Dodgson (1997), and shows

Table 1. Data points for the angular-size/redshift relationship; θ is in milliarcseconds.

z	
0.623	1.277
0.845	1.089
1.138	1.034
1.450	1.023
1.912	1.008
2.686	1.024

that the results obtained there were not spurious. Its purpose goes beyond that of showing compatibility with more recent work, and suggests that building a much larger angular-size/redshift data set for ultra-compact sources would be a promising enterprise. VLBI resolution of a quasar at $z = 5.82$ has been demonstrated (Frey et al 2003), so that the redshift limit of such a data set should go well beyond that expected of the Supernova/Acceleration probe (SNAP) (Aldering et al 2004), approaching 6 rather than 1.7. Additionally, this approach is immune to effects which might invalidate the SNe Ia results, such as absorption by grey dust, as has been noted by others (Bassett and Kunz 2004a; Bassett and Kunz 2004b). The two approaches are of course complementary in their redshift ranges, rather than competitive. Section 2 might act as a guide to further work, particularly with regard to the reduction of selection effects; additionally, samples might be filtered using morphological considerations, to include only those objects which show roughly circular symmetry, corresponding to the superimposed core/jet composites discussed in Section 2, which procedure would be similar to that adopted by Buchalter et al (1998) in their selection of FR-II sources. A related proposal due to Wiik and Valtaoja (2001) is that the linear sizes of shocks within jets might be estimated directly for each object, using flux density variations and light travel time arguments, so that each object would become a separate point in the angular-size/redshift diagram; a weakness in their case is that individual Doppler boosts have to be estimated.

I must end on a cautionary note; in general results from the 5 GHz sample due to Gurvits et al (1999) are compatible with the ones presented here, but with much greater uncertainty (Chen and Batra 2003); the prescription developed here does not significantly improve matters in this respect. The probable reason for this difference in behaviour is the definition of angular size; in Gurvits et al (1999) this is defined as the distance between the strongest component and the most distant one with peak brightness

2% of that of the strongest component; here the objective measure based upon fringe visibility ignores such outliers and estimates the size of the strongest component.

References

- Aldering G et al 2004 Preprint astro-ph/0405232
 Balbi A, Ade P, Bock J, Borrill J, Boscaleri A, De Bernardis P, Ferreira P G, Hanany S, Hristov V,

- Ja e A H, Lee A T, Oh S, Pascale E, Rabii B, Richards P L, Smoot G F, Stompor R, Winant C D and Wu J H P 2000 *Astrophys. J.* 545 L1
- Baldwin J E 1982 *Proc. IAU Symp.* 97 (Dordrecht: Reidel) p 21
- Barthel P D and Miley G K 1988 *Nature* 333 319
- Bassett B A and Kunz M 2004a *Astrophys. J.* 607 661
- Bassett B A and Kunz M 2004b *Phys. Rev. D* 69 101305
- Blandford R D, McKee C F and Rees M J, 1977 *Nature* 267 211
- Blandford R D and Königl A 1979a *Astrophys. Lett.* 20 15
- Blandford R D and Königl A 1979b *Astrophys. J.* 232 34
- Blundell K M and Rawlings S 1999 *Nature* 399 330
- Branch D, Livio M, Yungelson L R, Bo F R, Baron E and Baron E 1995 *Proc. Astronom. Soc. Pacific* 107 1019
- Bridle S L, Eke, V R, Lahav O, Lasenby A N, Hobson M P, Cole S, Frenk C S and Henry J P 1999 *Mon. Not. R. Astron. Soc.* 310 565
- Buchalter A, Helfand D J, Becker R H and White R L 1998 *Astrophys. J.* 494 503
- Chen G and Ratra B 2003 *Astrophys. J.* 582 586
- Cohen M H 1975 *Ann. N. Y. Acad. Sci.* 262 428
- Cohen M H, Mo et A T, Romney J D, Schilizzi R T, Seielstad G A, Kellermann K I, Purcell G H, Sha er D B, Pauliny-Toth I I K and Preuss E 1976 *Astrophys. J.* 206 L1
- Cohen M H, Lin eld R P, Mo et A T, Seielstad G A, Kellermann K I, Sha er D B, Pauliny-Toth I I K, Preuss E, W itzel A and Romney J D 1977 *Nature* 268 405
- Cunha J V, Alcaniz J S and Lima J A 2002 *Phys. Rev. D* 66 023520
- Dabrowski Y, Lasenby A and Saunders R 1995 *Mon. Not. R. Astron. Soc.* 277 753
- de Bernardis P et al 2000 *Nature* 404 955
- Efstathiou G, Sutherland W J and Maddox S J 1990 *Nature* 348 705
- Efstathiou G, Bridle S L, Lasenby A N, Hobson M P and Ellis R S 1999 *Mon. Not. R. Astron. Soc.* 303 L47
- Efstathiou G et al 2002 *Mon. Not. R. Astron. Soc.* 330 L29
- Fabian A C, Brandt W N, McMahon R G and Hook I M 1997 *Mon. Not. R. Astron. Soc.* 291 L5
- Fanaro B L and Riley J M 1974 *Mon. Not. R. Astron. Soc.* 167 31P
- Frey S and Gurvits L I 1977 *Vistas in Astronomy* 41 271
- Frey S, Gurvits L I, Kellermann K I, Schilizzi R T and Pauliny-Toth I I K 1997 *Astron. Astrophys.* 325 511
- Frey S, Moseni L, Paragiz and Gurvits L I 2003 *Mon. Not. R. Astron. Soc.* 343 L20
- Gilliland R L and Phillips M M 1998 *IAU Circ.* 6810
- Gurvits L I 1994 *Astrophys. J.* 425 442
- Gurvits L I, Schilizzi R T, Barthel P D, Kardashev N S, Kellermann K I, Lobanov A P, Pauliny-Toth I I K and Popov M V 1994 *Astron. Astrophys.* 291 737
- Gurvits L I, Kellermann K I and Frey S 1999 *Astron. Astrophys.* 342 378
- Hanany S et al 2000 *Astrophys. J.* 545 L5
- Hoyle F 1959 *Proc. IAU Symp.* 9: Paris Symposium on Radio Astronomy (Stanford: Stanford University Press) p 529
- Jackson J C 1973 *Mon. Not. R. Astron. Soc.* 162 11P
- Jackson J C and Dodgson M 1996 *Mon. Not. R. Astron. Soc.* 278, 603
- Jackson J C and Dodgson M 1997 *Mon. Not. R. Astron. Soc.* 285, 806
- Jain D, Dev A and Alcaniz J S 2003 *Class. Quant. Grav.* 20 4485
- Kembhavi A K and Narlikar J V 1999 *Quasars and Active Galactic Nuclei* (Cambridge: Cambridge University Press) chapter 9
- Kellermann K I 1972 *Astronom. J.* 77 531
- Kellermann K I 1993 *Nature* 361 134
- Kellermann K I 1994 *Aust. J. Phys.* 47 599

- Kormendy J 2001a *ASP Conf. Ser.* 230: Galaxy Disks and Disk Galaxies (San Francisco: Astronomical Society of the Pacific) p 247
- Kormendy J 2001b *Rev. Mex. Astron. Astrofis. (Serie de Conferencias)* 10 69
- Larsenby A N, Bridle S L and Hobson M P 2000 *Astrophys. Lett. & Communications* 37 327
- Legg T H 1970 *Nature* 226 65
- Lind K R and Blandford R D 1985 *Astrophys. J.* 295 358
- Livio M 2001 *Proc. STScI Symp. 13: Supernovae and Gamma-Ray Bursts* (Cambridge: Cambridge Univ. Press) p 334
- Lin J A S and Aikani J S 2002 *Astrophys. J.* 566 15
- Masson C R 1980 *Astrophys. J.* 242 8
- Miley G K, 1971 *Mon. Not. R. Astron. Soc.* 152 477
- Nilsson K, Valtonen M J, Kotilainen J and Jaakkola T 1993 *Astrophys. J.* 413 453
- Orr M J L and Browne I W A 1982 *Mon. Not. R. Astron. Soc.* 200 1067
- Ostriker J P and Steinhardt P J 1995 *Nature* 377 600
- Padovani P and Urry C M 1990 *Astrophys. J.* 356 75
- Paragiz, Frey S, Gurvits L I, Kellermann K I, Schilizzi R T, McMahon R G, Hook I M and Pauliny-Toth I I K 1999 *Astron. Astrophys.* 344 51
- Peebles P J E 1984 *Astrophys. J.* 284 439
- Perlmutter S et al 1999 *Astrophys. J.* 517 565
- Press W H, Flannery B P, Teukolsky S A and Vetterling W T 1986, *Numerical Recipes* (Cambridge: Cambridge University Press) pp 532-536
- Preston R A, Morabito D D, Williams J G, Faulkner J, Jauncey D L, Nicolson G 1985 *Astronom. J.* 90 1599
- Readhead A C S, Taylor G B, Xu W, Pearson T J, Wilkinson P N, Polatidis A G 1996a *Astrophys. J.* 460 612
- Readhead A C S, Taylor G B, Pearson T J, Wilkinson P N 1996b *Astrophys. J.* 460 634
- Rees M 1966 *Nature* 211 468
- Richter G M 1973 *Astrophys. Lett.* 13 63
- Reiss A G, Filippenko A V, Challis P, Ciochiatti A, Diercks A, Gamavich P M, Gilliland R L, Hogan C J, Jha S, Kirshner R P, Leibundgut B, Phillips M M, Reiss D, Schmidt B P, Schommer R A, Smith R C, Spyromilio J, Stubbs C, Suntze N B and Tonry J 1998 *Astronom. J.* 116 1009
- Reiss A G, Nugent P E, Gilliland R L, Schmidt B P, Tonry J, Dickinson M, Thompson R I, Budavari T, Casertano S, Evans S, Filippenko A V, Livio M, Sanders D B, Shapley A E, Spinrad H, Steidel C C, Stern D, Surace J and Veilleux S 2001 *Astrophys. J.* 560 49
- Scheuer P G A and Readhead A C S 1979 *Nature* 277 182
- Schmidt B P et al 1998 *Astrophys. J.* 507 46
- Shklovsky I S 1964a *Soviet Astron.* (AJ) 7 748
- Shklovsky I S 1964b *Soviet Astron.* (AJ) 7 972
- Singal A K 1988 *Mon. Not. R. Astron. Soc.* 233 87
- Spergel D N, Verde L, Peiris H V, Komatsu E, Nolte M R, Bennett C L, Halpern M, Hinshaw G, Jarosik N, Kogut A, Limon M, Meyer S S, Page L, Tucker G S, Weiland J L, Wollack E and Wright E L 2003 *Astrophys. J. Suppl.* 148 175
- Taylor G B, Vermeulen R C, Readhead A C S, Pearson T J, Henstock D R, and Wilkinson P N 1996 *Astrophys. J. Suppl.* 107 37
- Thompson A R, Moran J M and Swenson G W Jr 1986 *Interferometry and Synthesis in Radio Astronomy* (New York: Wiley) p 13
- Turner M S, Steigman G and Krauss L L 1984 *Phys. Rev. Lett.* 52 2090
- Vishwakarma R G 2001 *Class. Quant. Grav.* 18 1159
- Wardle J F C and Miley G K 1974 *Astron. Astrophys.* 30 305
- Wilk K and Valtaoja E 2001 *Astron. Astrophys.* 366 1061
- Wilkinson P N, Polatidis A G, Readhead A C S, Xu W and Pearson T J, 1994 *Astrophys. J.* 432 L87

5. Figures

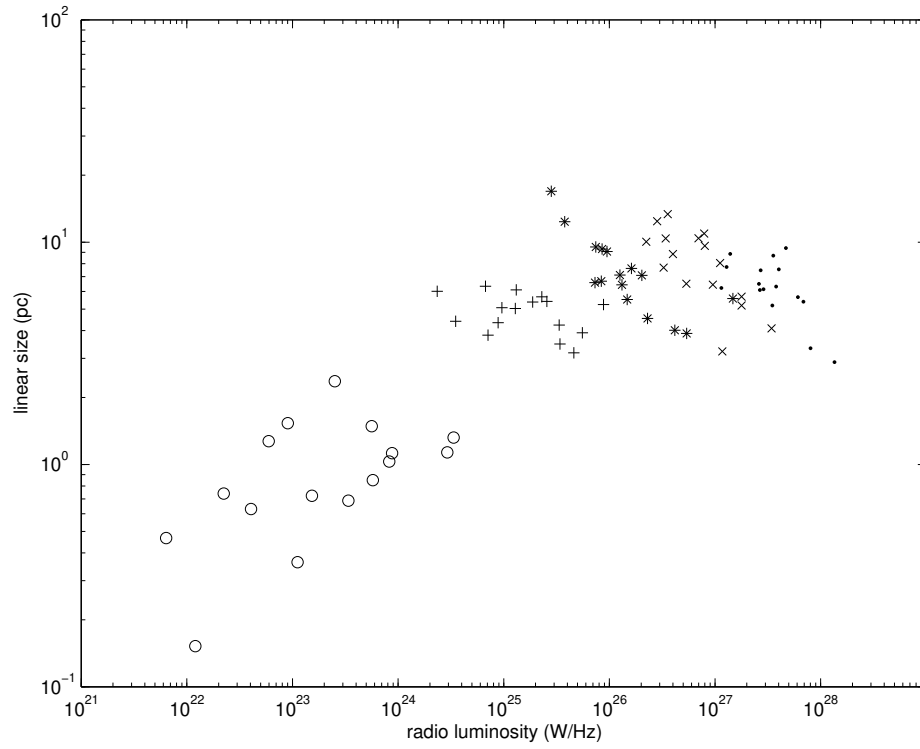


Figure 1. Linear size versus radio luminosity for sources in selected redshift bins: $0.00 < z < 0.06$, $0.21 < z < 0.31$, $0.51 < z < 0.58$, $1.15 < z < 1.29$, $2.70 < z < 3.79$, showing the inverse correlation between linear size and radio power at high redshifts.

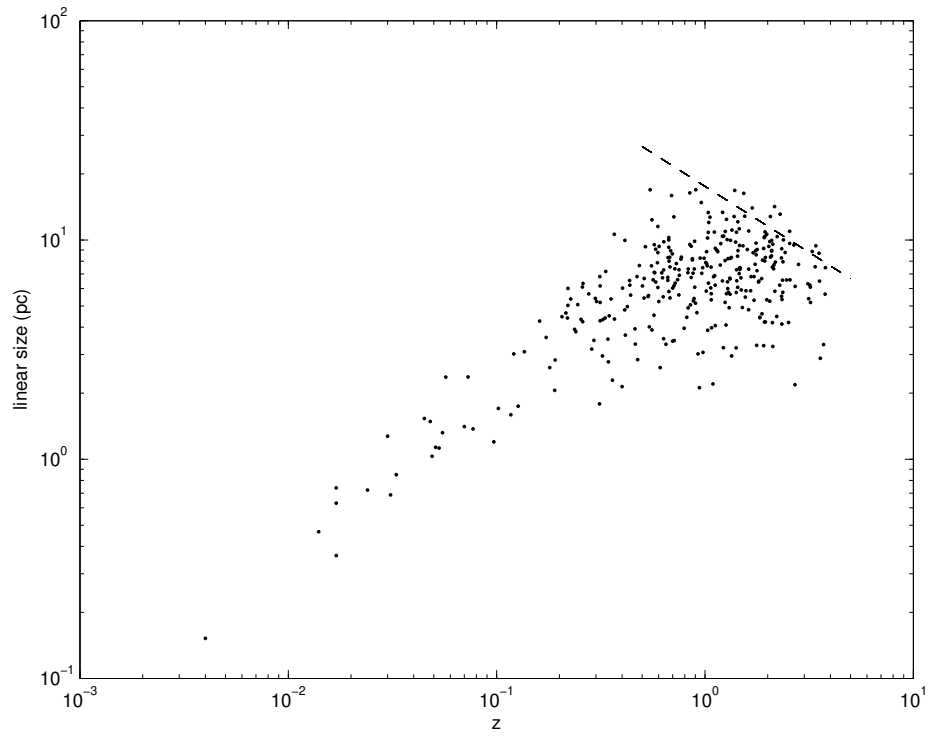


Figure 2. Linear size versus redshift for the 337 sources in the sample used here. The dashed cut-off curve corresponds to the model discussed in the text, in which larger sources are intrinsically weaker.

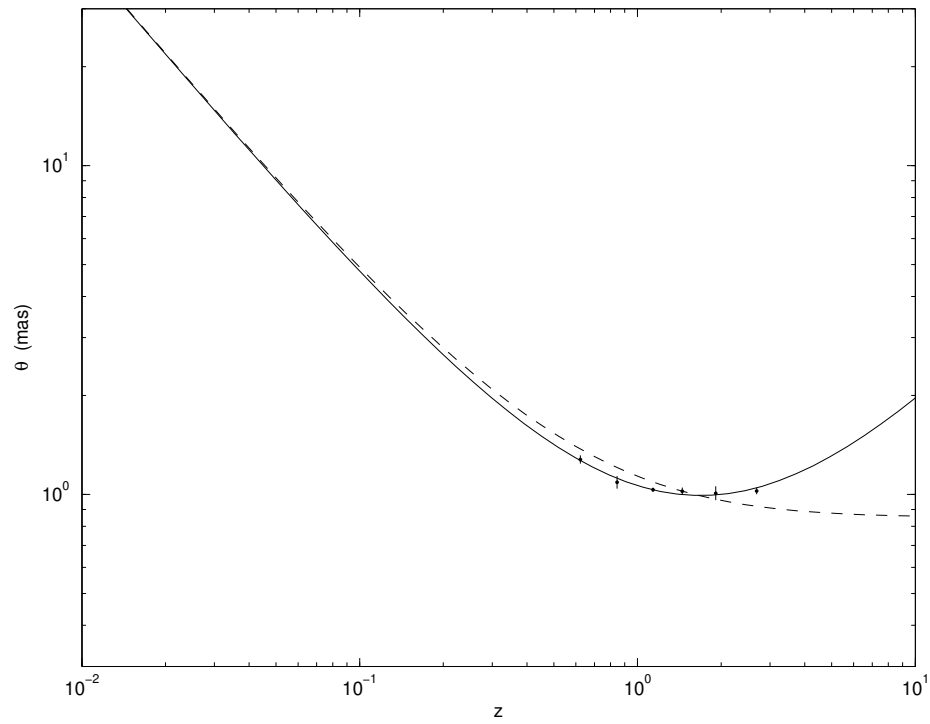


Figure 3. Angular size versus redshift for 252 sources with $0.541 \leq z \leq 3.787$, divided into 6 bins of 42 objects; $|m| = 0.24$, $n = 0.76$; ---- $m = 0$, $n = 0$. The angular size corresponds roughly to the 14th object within each bin; this definition is used to reduce the effects of bias against large objects, see text.

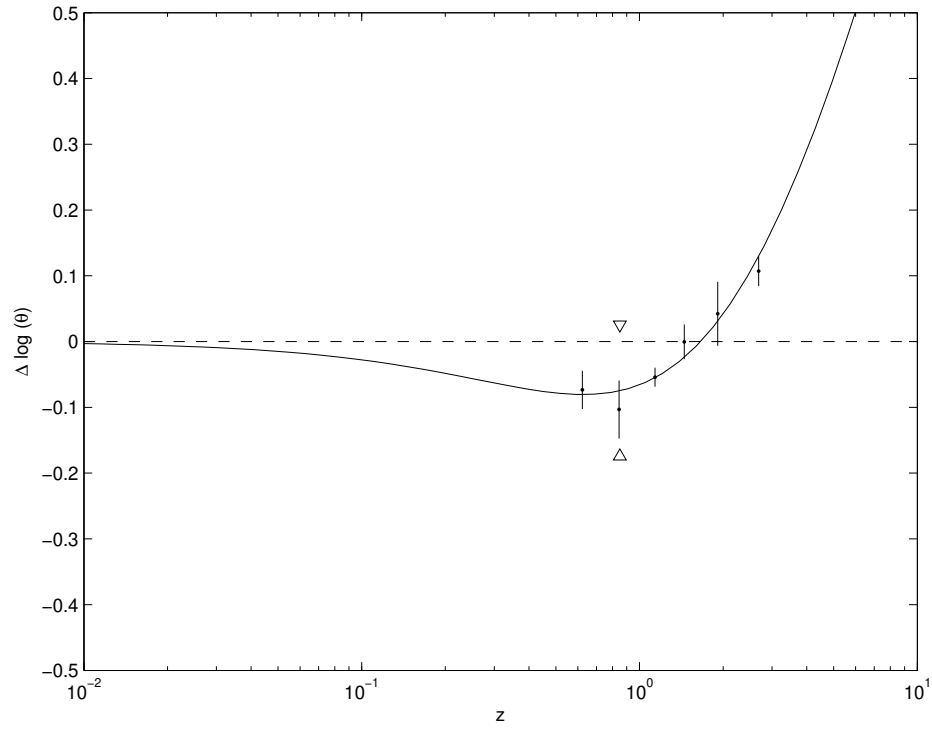


Figure 4. Differential form of Figure 3; $| \quad | \quad m = 0.24, \quad = 0.76$; ---- $m = 0, \quad = 0$; the triangles delineate the transition from acceleration to deceleration, at $z = 0.85$.

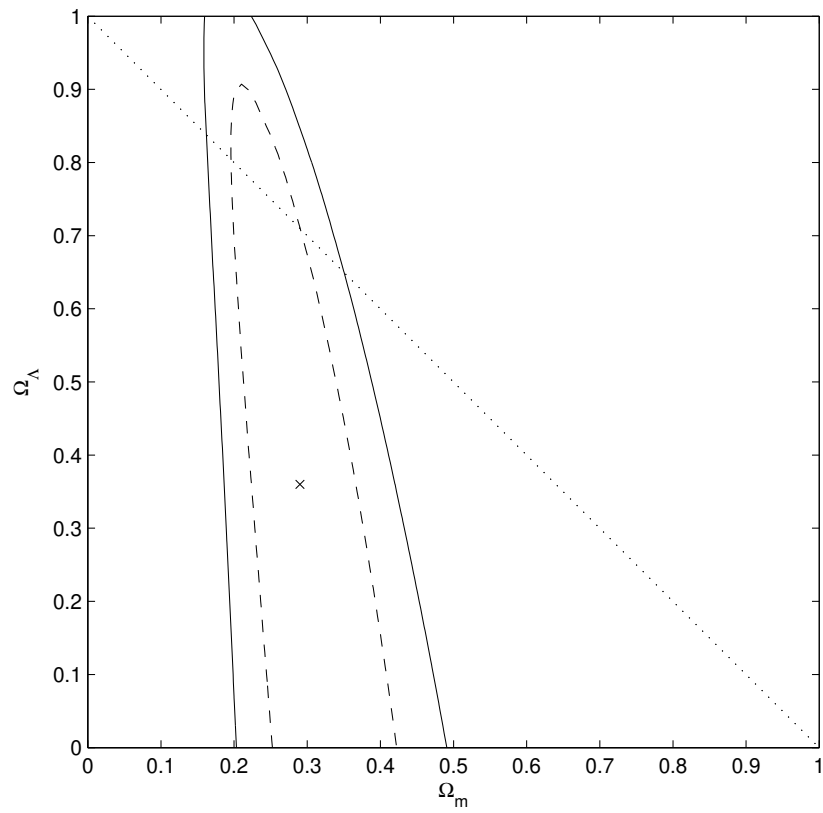


Figure 5. Confidence regions in the Ω_m - Ω_v plane, marginalised over the linear dimension d ; — 95%, --- 68%, linear dimension d . The cross indicates the global minimum in χ^2 , at $\Omega_m = 0.29$, $\Omega_v = 0.37$.

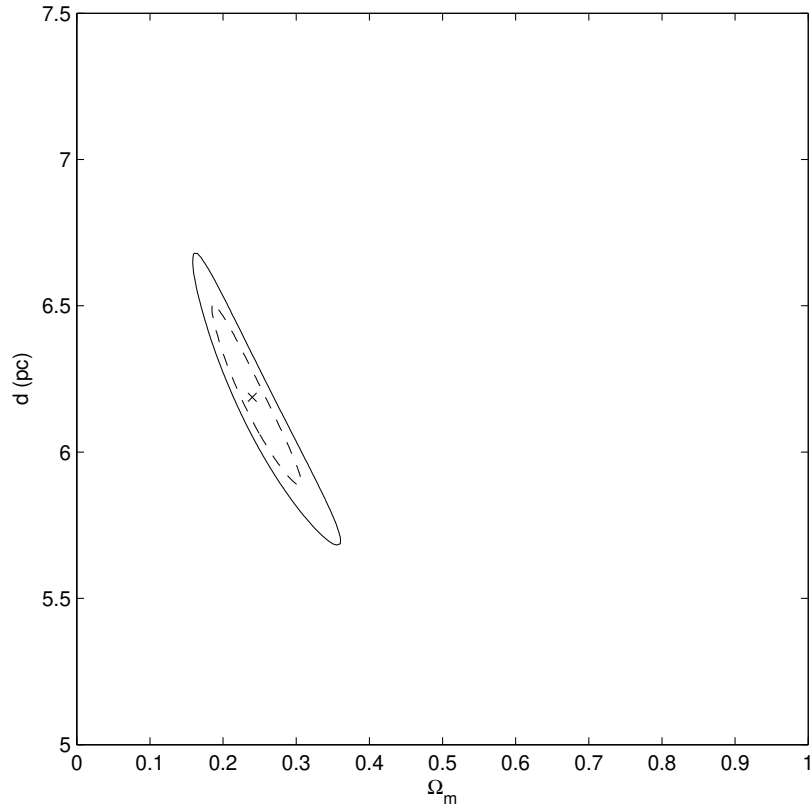


Figure 6. Confidence regions in the Ω_m - d plane for Λ CDM models; $| |$ 95%, $---$ 68%. The cross indicates the global minimum in χ^2 , at $\Omega_m = 0.24$, $d = 6.20$ pc. Marginalising over the linear dimension d gives $\Omega_m = 0.24 \pm 0.09 = 0.07$.

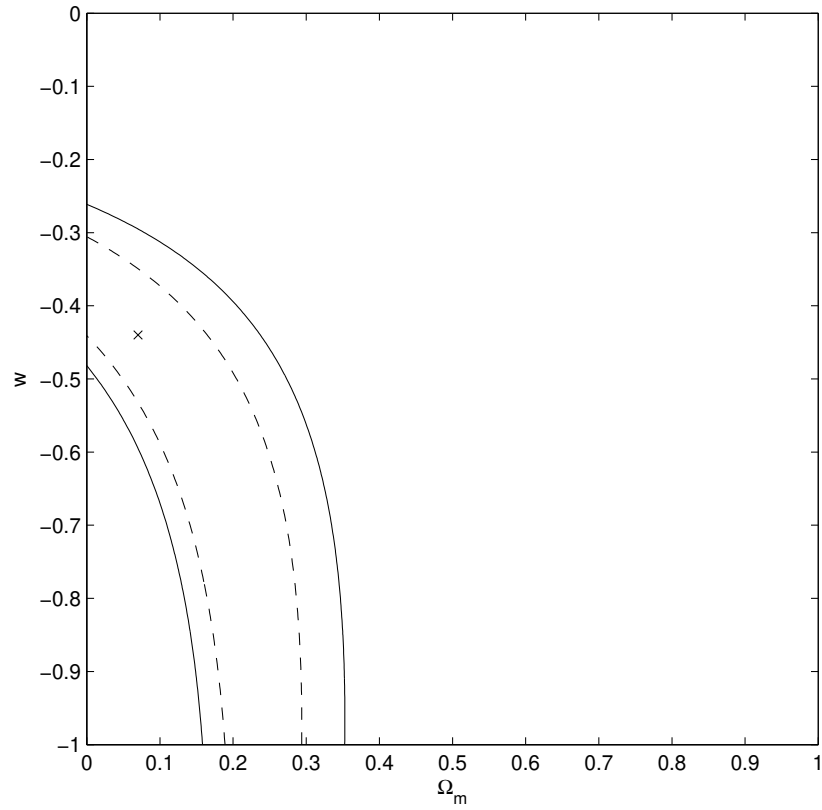


Figure 7. Confidence regions in the Ω_m - w plane for flat models, marginalised over the linear dimension d , where w is the quintessence parameter; $—$ 95%, $- - -$ 68%. The cross indicates the global minimum in χ^2 , at $\Omega_m = 0.07$, $w = -0.44$.